Supporting Information

A Contact-Polymerizable Hemostatic Powder for Rapid Hemostasis

Jia Wang[ab], Cheng Li[bc], Wei Zhang[b], Weimin Huang[b], Zhiqiang Liu[d], Rui Shi[e], Shiyuan Wang[b], Shan Liu[f], Weiguo Shi[b], Yunlan Li[a], Liang Xu[b]*.*

[a] School of Pharmaceutical Science, Shanxi Medical University, 56 Xinjian South Road, Taiyuan, 030001, China.
[b] State Key Laboratory of Toxicology and Medical Countermeasures, Beijing Institute of Pharmacology and Toxicology, 27 Taiping road, Beijing, 100850, China.
[c] Department of Orthopaedic Surgery, Beijing Jishuitan Hospital, Fourth Clinical College of Peking University, Beijing, China
[d] Beijing Institute of Basic Medical Sciences, 27 Taiping road, Beijing, 100850, China.
[e] Beijing Research Institute of Traumatology and Orthopaedics, Beijing Jishuitan Hospital, Beijing, 100035, China.
[f] Pathology Department of PLA Rocket Force Characteristic Medical Center, Beijing 100085, China
[*] Corresponding author

Synthesis of the CA–PEG–CA

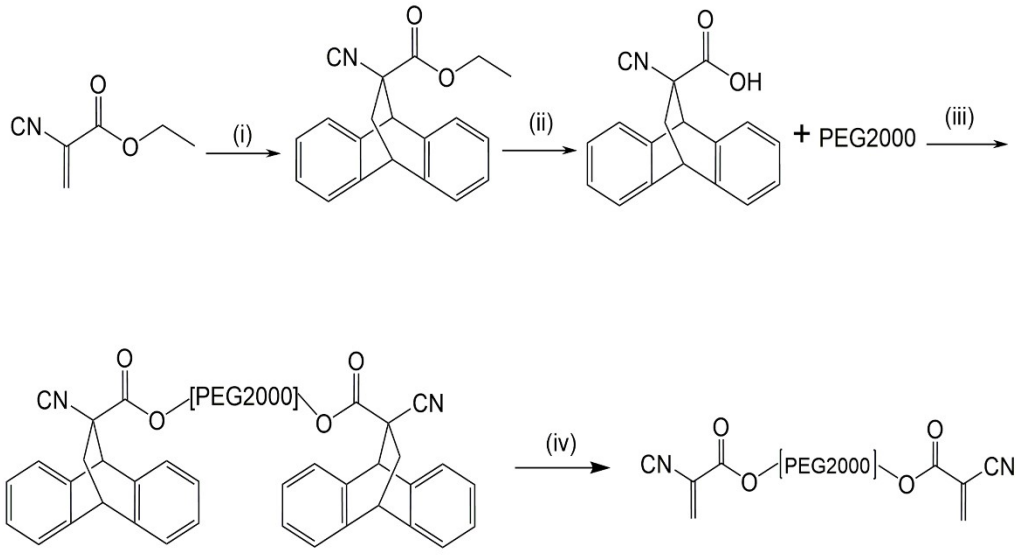

Scheme S1. Synthetic route of CA-PEG-CA（i）toluene, rt.（ii）ethanol,KOH,H_2O,rt, 78.8%. (iii) PEG2000, DMAP, DIC, DCM, dichloromethane, rt, 67.3% (iv)maleic anhydride, dimethylbenzene, rt, 63.9%.

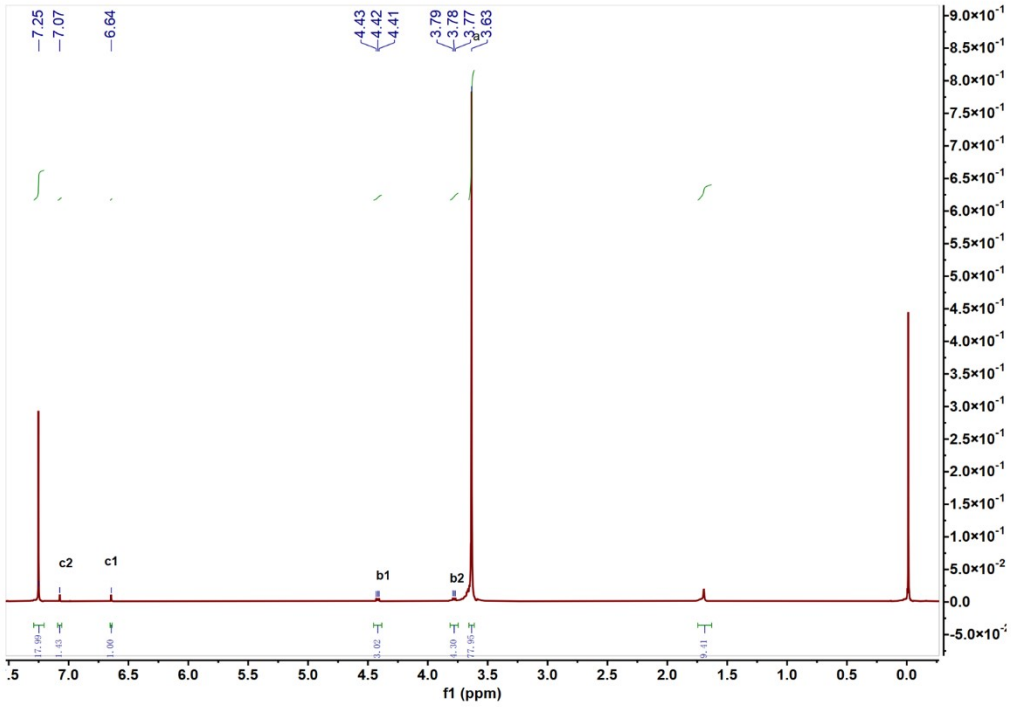

Fig. S1 1H NMR spectra of monomer compound of poly(ethylene glycol)–di(cyanoacrylate) (CA–PEG–CA)

1H-NMR (400 MHz, CDCl3, 25 1C, TMS): d 7.09 (s, 2H, H 2CQC), 6.66 ppm (s, 2H, H 2CQC), 4.43 ppm (t, 3J(H,H) = 8.3 Hz, 4H; COO CH2), 3.68 ppm (m, 232H; O CH2 CH2).

The Swelling Ratio in Deionized water and Tap water

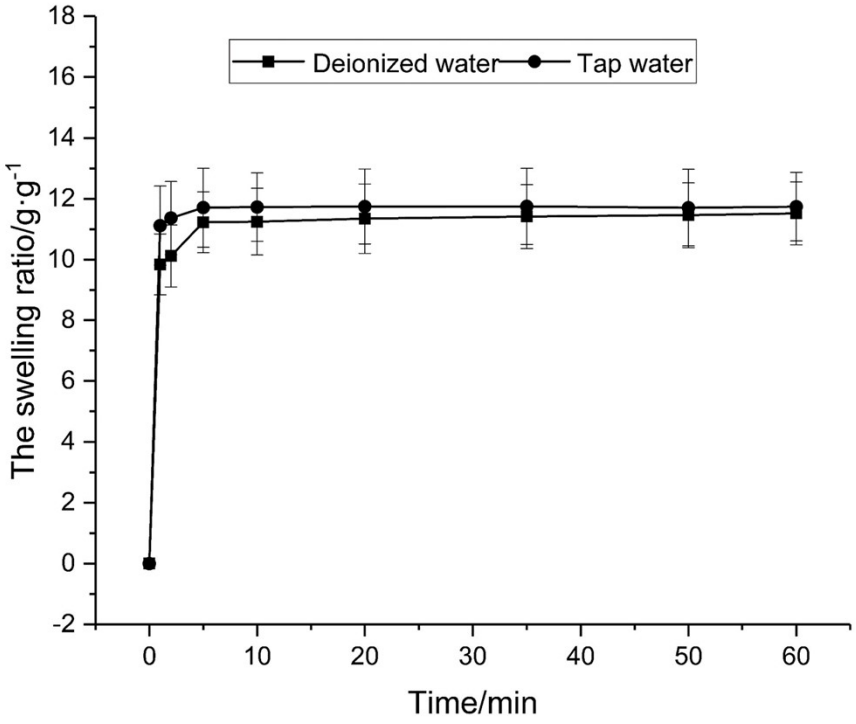

Fig S2. The swelling ratio in deionized water and tap water of the CA-PEG-CA powder.

Clotting Mechanism

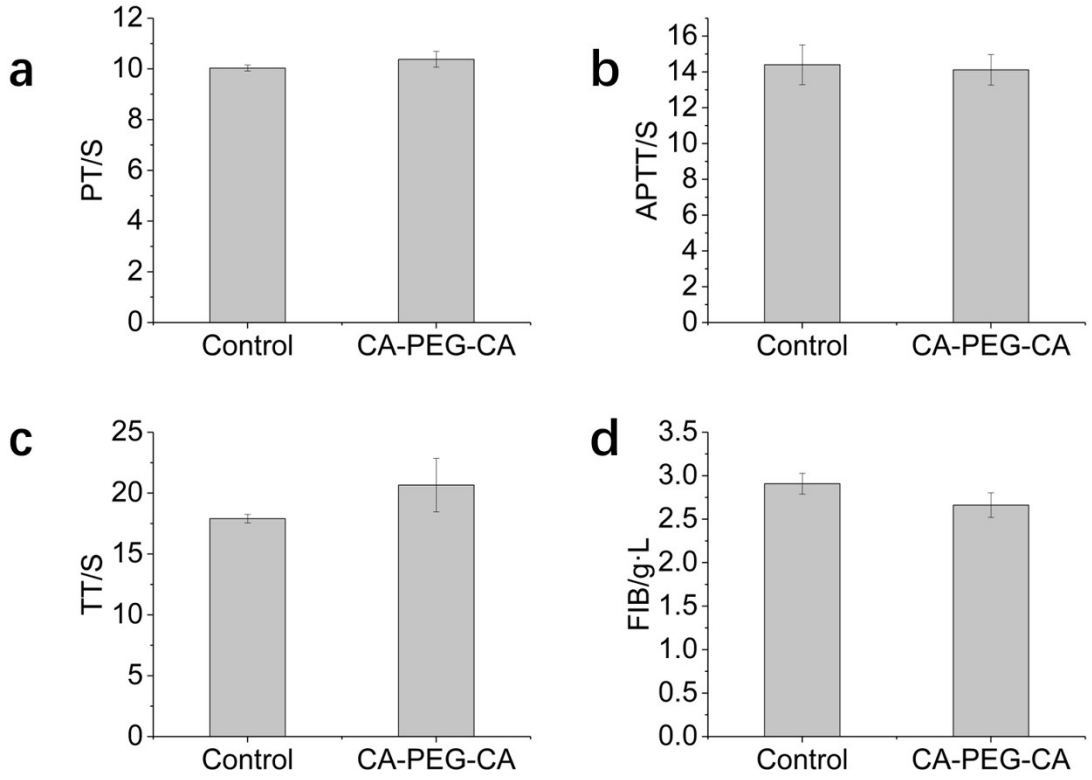

Fig. S3 The four coagulation items assay of the CA-PEG-CA powder

Antibacterial Property

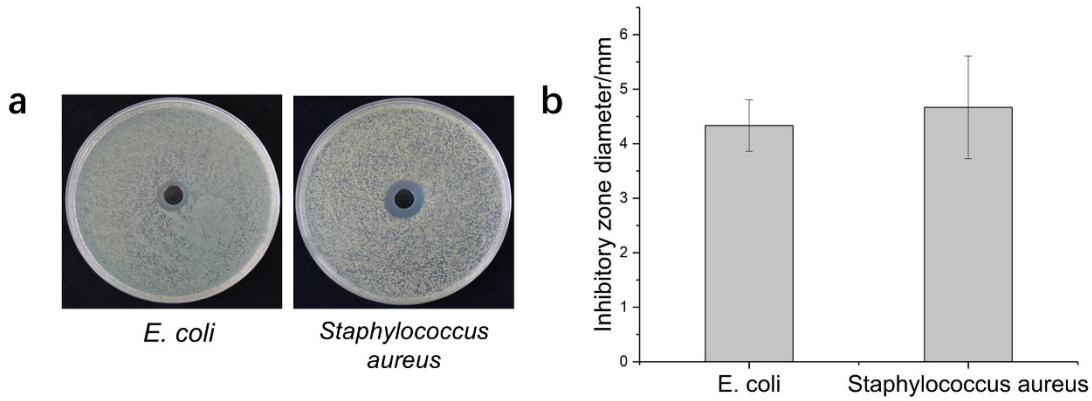

Fig S4. Antibacterial property of the CA-PEG-CA. (a, b) Bacteriostatic zone test and the size of bacteriostatic zone diameter of E. coli and S. aureus co-cultured with the CA-PEG-CA powder.

Rat liver hemorrhage model

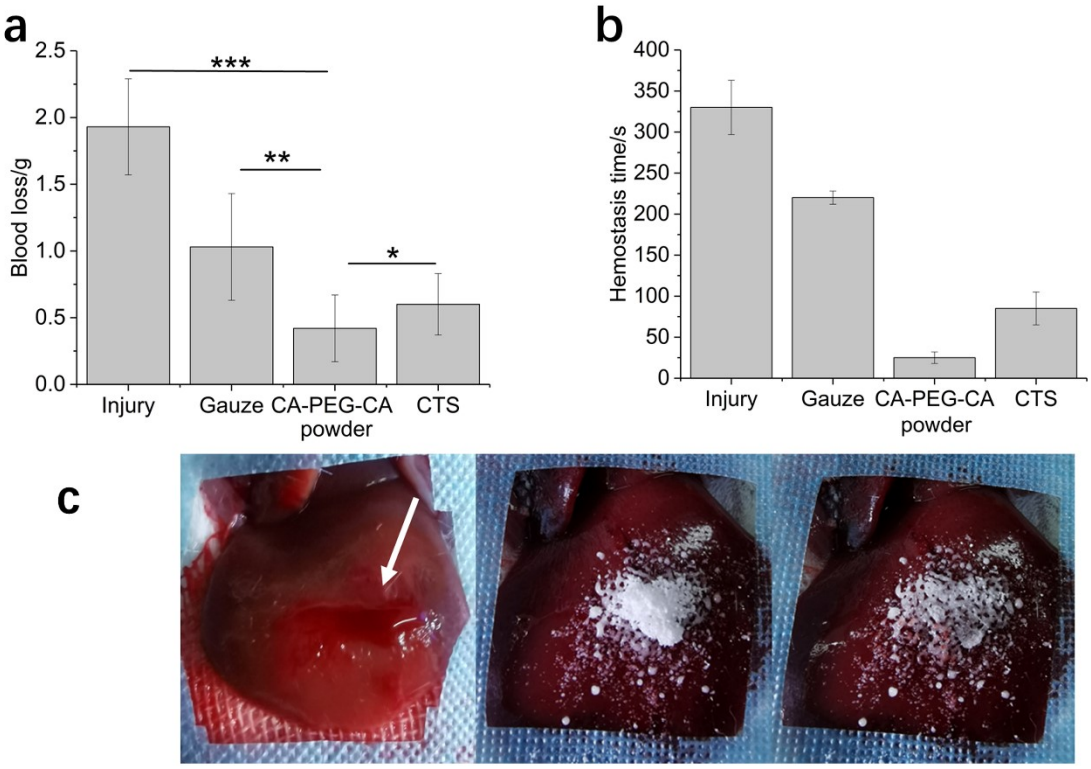

Fig. S5. In vivo hemostatic performances in rat liver hemorrhage model. (a, b) The blood loss and hemostasis time of CA-PEG-CA in rat liver injury hemorrhage model, compared with that of the commercialized chitosan. c) The bleeding experiment photos. Error bars represent the s. d. of six independent experiments. *$p < 0.05$, **$p < 0.01$, ***$p < 0.001$.

Rat spleen hemorrhage model

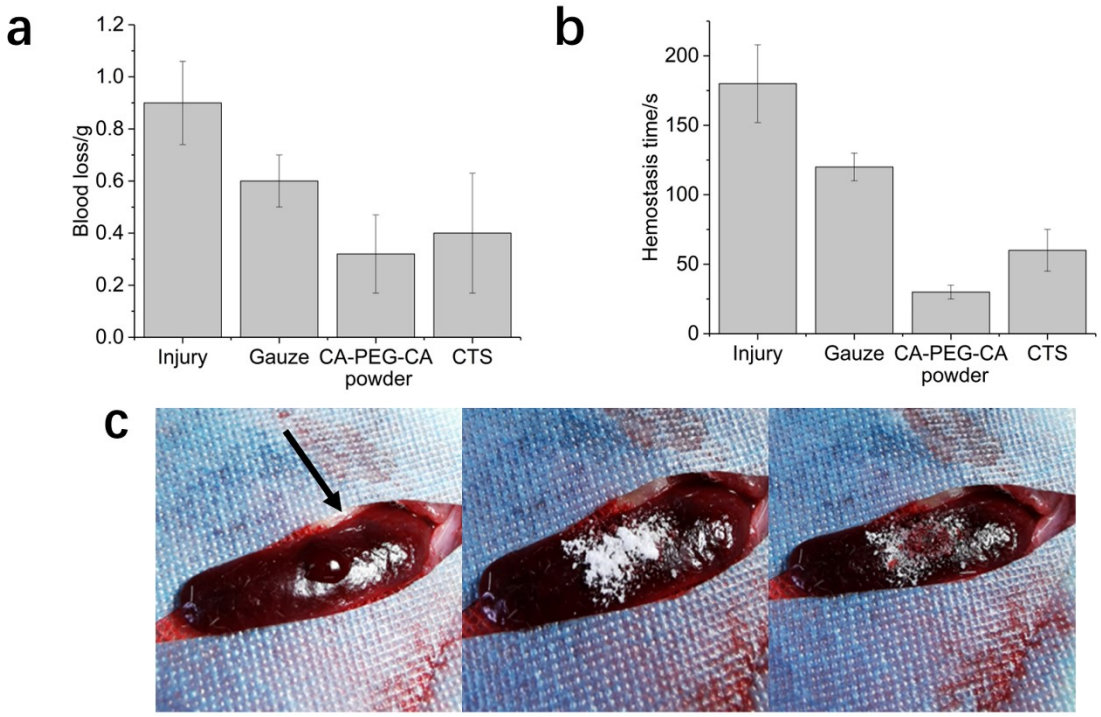

Fig. S6 In vivo hemostatic performances in rat spleen hemorrhage model. (a, b) The blood loss and hemostasis time of CA-PEG-CA in rat spleen injury hemorrhage model, compared with that of the commercialized chitosan. c) The bleeding experiment photos. Error bars represent the s. d. of six independent experiments. *$p < 0.05$, **$p < 0.01$, ***$p < 0.001$.

Rat kidney hemorrhage model

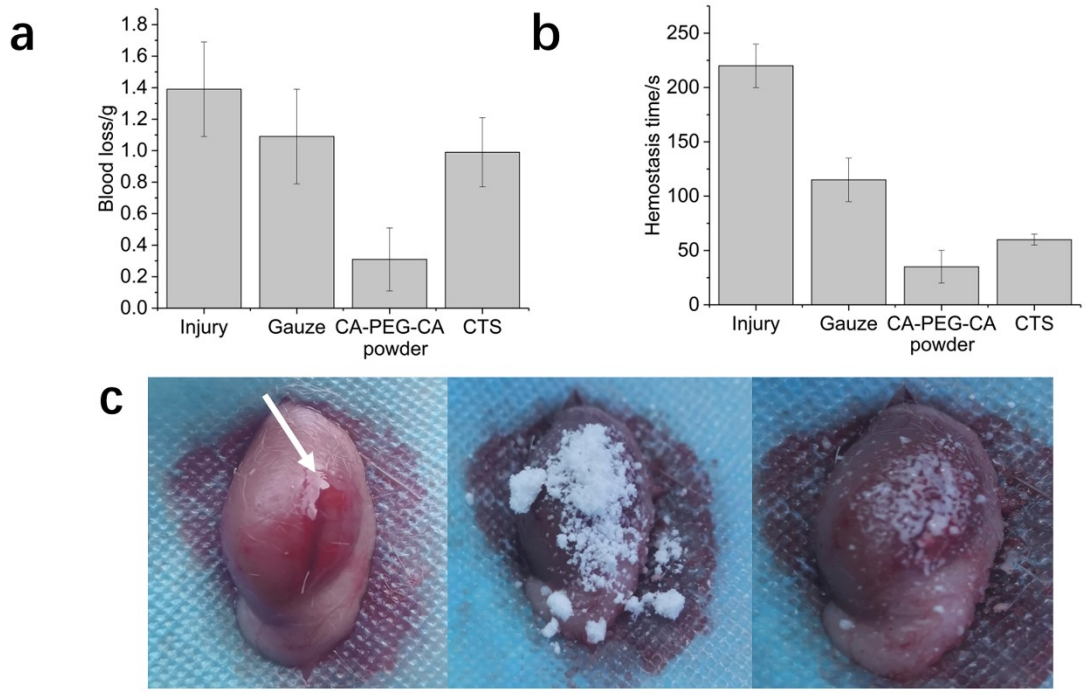

Fig. S7 In vivo hemostatic performances in rat kidney hemorrhage model. (a, b) The blood loss and hemostasis time of CA-PEG-CA in rat kidney hemorrhage model, compared with that of the commercialized chitosan. c) The bleeding experiment photos. Error bars represent the s. d. of six independent experiments. *$p < 0.05$, **$p < 0.01$, ***$p < 0.001$.

Degradation Experiments

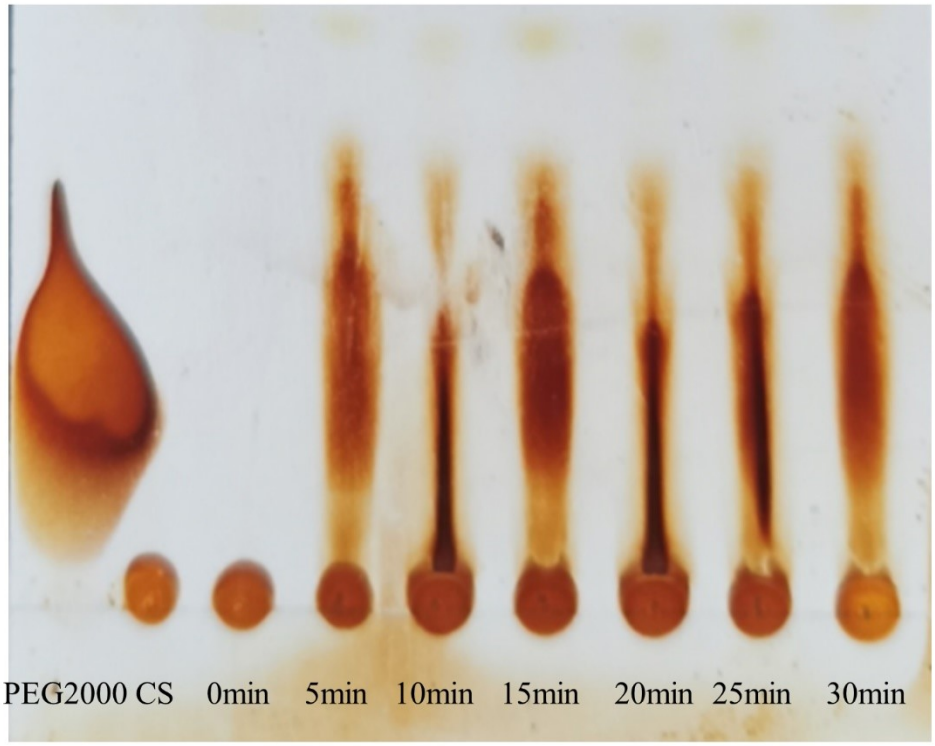

Fig. S8 Thin layer chromatography of PEG2000 with degradation time

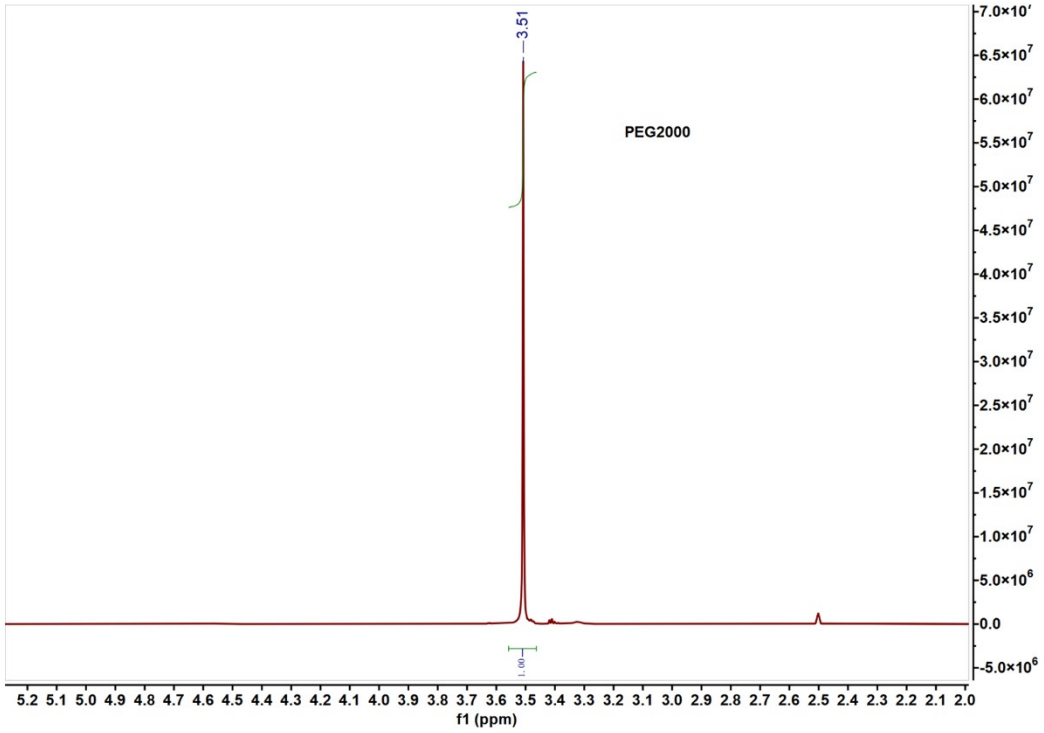

Fig. S9 ^{1}H NMR spectra of the degradation product catalyzed by CS in CDCl3.

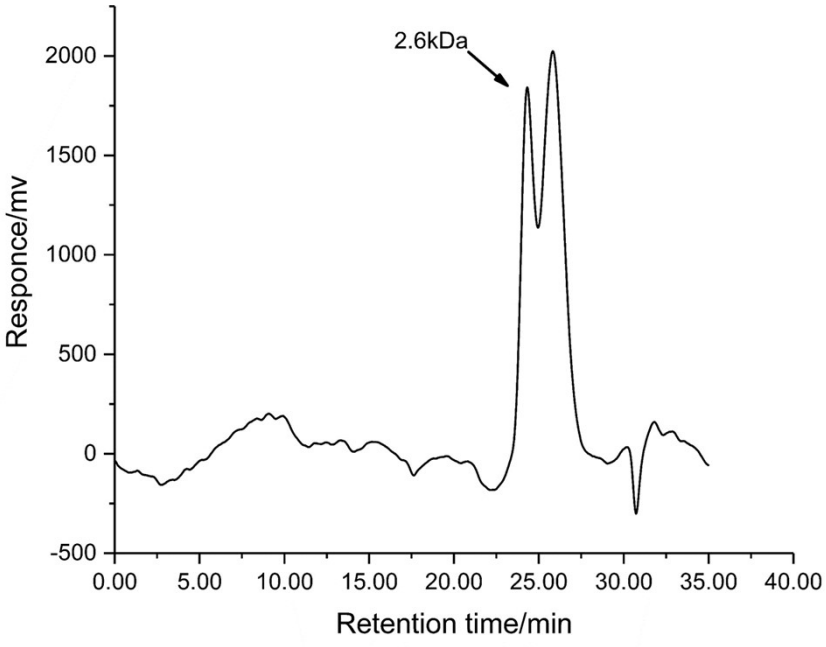

Fig. S10 Aqueous Gel Permeation Chromatography of the degradation product catalyzed by CS

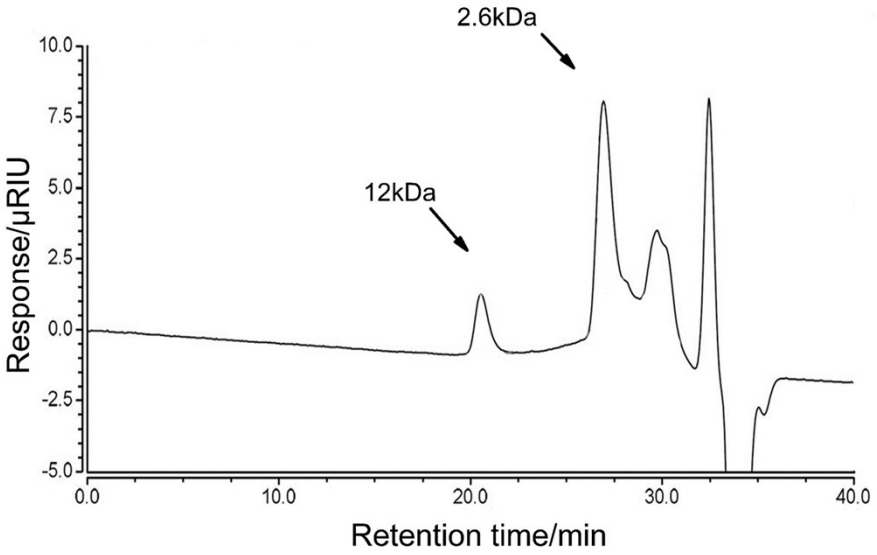

Fig. S11 Organic Gel Permeation Chromatography of the degradation product catalyzed by CS